

## Modulating the nucleophile of a glycoside hydrolase through site-specific incorporation of fluoroglutamic acids

Miriam P. Koetzler, Kyle Robinson, Hong-Ming Chen, Mark Okon, Lawrence P. McIntosh, and Stephen G. Withers

*J. Am. Chem. Soc.*, **Just Accepted Manuscript** • DOI: 10.1021/jacs.8b04235 • Publication Date (Web): 12 Jun 2018

Downloaded from <http://pubs.acs.org> on June 12, 2018

### Just Accepted

“Just Accepted” manuscripts have been peer-reviewed and accepted for publication. They are posted online prior to technical editing, formatting for publication and author proofing. The American Chemical Society provides “Just Accepted” as a service to the research community to expedite the dissemination of scientific material as soon as possible after acceptance. “Just Accepted” manuscripts appear in full in PDF format accompanied by an HTML abstract. “Just Accepted” manuscripts have been fully peer reviewed, but should not be considered the official version of record. They are citable by the Digital Object Identifier (DOI®). “Just Accepted” is an optional service offered to authors. Therefore, the “Just Accepted” Web site may not include all articles that will be published in the journal. After a manuscript is technically edited and formatted, it will be removed from the “Just Accepted” Web site and published as an ASAP article. Note that technical editing may introduce minor changes to the manuscript text and/or graphics which could affect content, and all legal disclaimers and ethical guidelines that apply to the journal pertain. ACS cannot be held responsible for errors or consequences arising from the use of information contained in these “Just Accepted” manuscripts.

# Modulating the nucleophile of a glycoside hydrolase through site-specific incorporation of fluoroglutamic acids

Miriam P. Kötzler<sup>1</sup>, Kyle Robinson<sup>1</sup>, Hong-Ming Chen<sup>1</sup>, Mark Okon<sup>1,2</sup>, Lawrence P. McIntosh<sup>1,2,3</sup> and Stephen G. Withers<sup>1,2\*</sup>

<sup>1</sup>Department of Chemistry, <sup>2</sup>Department of Biochemistry and Molecular Biology, <sup>3</sup>Michael Smith Laboratories, University of British Columbia, Vancouver, BC, Canada V6T 1Z1

**Keywords:** *Bacillus circulans* endo- $\beta$ -1,4-xylanase, nucleophilic catalysis, 4-fluoroglutamic acid, 4,4-difluoroglutamic acid, protein semisynthesis, unnatural amino acid, linear free energy relationship, enzyme engineering.

---

**ABSTRACT:** Understanding the detailed mechanisms of enzyme-catalyzed hydrolysis of the glycosidic bond is fundamentally important, not only to the design of tailored cost-efficient, stable and specific catalysts, but also to the development of specific glycosidase inhibitors as therapeutics. Retaining glycosidases employ two key carboxylic acid residues, typically glutamic acids, in a double-displacement mechanism involving a covalent glycosyl-enzyme intermediate. One Glu functions as a nucleophile while the other acts as a general acid/base. A significant part of enzymatic proficiency is attributed to a “perfect match” of the electrostatics provided by these key residues, a hypothesis that has been remarkably difficult to prove in model systems or in enzymes themselves. We experimentally probe this synergy by preparing synthetic variants of a model glycosidase, *Bacillus circulans*  $\beta$ -xylanase (Bcx) with the nucleophile Glu78 substituted by 4-fluoro or 4,4-difluoroglutamic acid to progressively reduce nucleophilicity. These Bcx variants were semi-synthesized by preparation of optically pure fluoroglutamic acid building blocks, incorporation into synthetic peptides and ligation onto a truncated circular permutant of Bcx. By measuring the effect of altered electrostatics in the active site on enzyme kinetic constants, we show that lowering the nucleophile pK<sub>a</sub> by two units shifts the pH-dependent activity by one pH unit. Linear free energy correlations using substrates of varying leaving group ability indicate that by reducing nucleophilic catalysis, the concerted mechanism of the enzyme is disrupted and shifted towards a dissociative pathway. Our study represents the first example of site-specific introduction of fluorinated glutamic acids into any protein. Furthermore, it provides unique insights into the synergy of nucleophilic and acid/base catalysis within an enzyme active site.

---

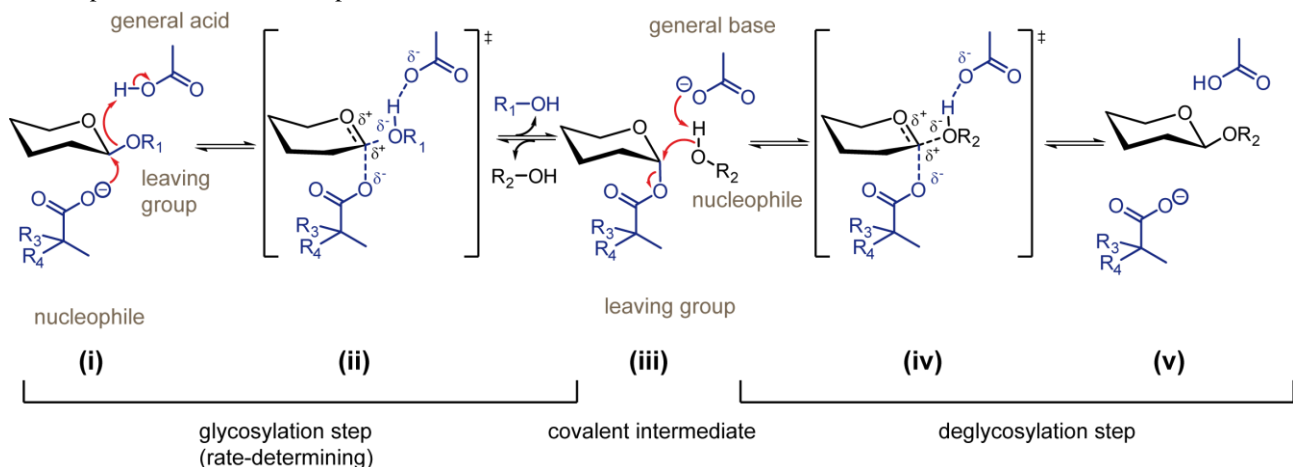
## Introduction

Glycoside hydrolases are among the most proficient catalysts known, accelerating reactions by up to  $\sim 10^{17}$  fold above the sluggish, uncatalyzed processes.<sup>1</sup> They are also among the most widely used enzymes commercially, with applications ranging from food processing and brewing through to the textiles, biofuel and pulp and paper industries.<sup>2-5</sup> Some of these enzymes, among them the *Bacillus circulans* endo- $\beta$ -1,4-xylanase (Bcx), have been engineered to optimize their stability and activity for use under harsh processing conditions.<sup>4,6,7</sup> Further fine-tuning of catalytic properties, including shifting or broadening pH-dependent activity profiles, would be of great interest. However, this requires a deep mechanistic understanding of factors underlying catalysis, such as protonation equilibria in the active site and electrostatic stabilization of the transition states.

The general models of catalytic mechanisms employed by glycoside hydrolases were introduced by Koshland over half a century ago<sup>8</sup> and have been heavily refined in the interim.<sup>9,10</sup> Inverting glycoside hydrolases (which effect inversion of anomeric stereochemistry) employ a direct displacement mechanism via a single oxocarbenium-like transition state. By contrast retaining glycoside hydrolases use a two-step mechanism involving two oxocarbenium-like transition states (ii and iv in Scheme 1). One carboxylate (Glu78 in Bcx) acts as a nucleophilic catalyst, attacking the anomeric carbon to form a covalent glycosyl enzyme intermediate (glycosylation step (i) to (ii)). This transient covalent intermediate (iii) is then hydrolyzed in the second step, releasing the free reducing sugar with net retention of anomeric configuration (deglycosylation step (iv) to (v)). The second carboxylic acid (Glu172 in Bcx) acts as a general acid catalyst in the first step, transferring a proton onto the glycosidic oxygen as the nucleophile attacks and thereby enhancing the leaving group ability of an otherwise unactivated aglycone (leaving group pK<sub>a</sub>  $\sim 16$  for a sugar alcohol). Upon formation of the covalent glycosyl enzyme intermediate and ablation of the charge on the nucleophilic carboxyl, the pK<sub>a</sub> of the acid/base residue drops. This sets the carboxyl group in its deprotonated form, enabling it to function as the base catalyst in the second step and deprotonate, in a concerted fashion, a water molecule that attacks the anomeric carbon.<sup>11</sup> Beyond the well-established framework of this double-displacement mechanism, a deep understanding of how the  $10^{17}$  fold rate enhancement is achieved, or how the pH optimum of a

glycoside hydrolase is set, remains to be fully established. However, computational approaches are contributing to addressing these fundamental questions.<sup>12,13</sup>

Central to this desired understanding is the nature of the interplay between the two key catalytic carboxylic acids, a phenomenon that is challenging to study experimentally. In contrast to what is seen for spontaneous hydrolysis of glycosides in aqueous solution, enzymatic cleavage proceeds through steps involving concerted proton transfers. In Bcx, the first step (glycosylation) is rate-limiting in  $k_{\text{cat}}$  and  $k_{\text{cat}}/K_M$ , even for aryl glycosides.<sup>14</sup> Thus the stability of the first transition state relative to the ES complex or free enzyme, respectively, determines the observed rates of hydrolysis. As shown by NMR-monitored titrations of selectively <sup>13</sup>C-labelled Bcx, the protonation equilibria of Glu78 and Glu172 in the free enzyme are responsible for the observed profile of  $k_{\text{cat}}/K_M$  vs pH, which is bell-shaped with a maximum at pH 5.9.<sup>11,15</sup>



**Scheme 1: Mechanism of retaining glycoside hydrolases. Hydrolysis of the glycosidic bond proceeds via two oxocarbenium ion-like transition states, stabilized by two carboxylic acid/carboxylate residues. In Bcx, the first step is rate-limiting. Modification of the 4-position of the catalytic nucleophile Glu78 (R<sub>3</sub>, R<sub>4</sub>) will therefore modulate initial protonation equilibria, as well as charge distribution at the transition states.**

The nature of transition state (ii) is not intuitive, since carboxylate anions are poor nucleophiles in water and the anomeric carbon is likewise weakly electrophilic.<sup>16</sup> Furthermore, proton transfer from a weak acid ( $pK_a$  Glu172 = 6.7) to a weakly basic exocyclic oxygen is thermodynamically unfavorable.<sup>17–19</sup> It is the interplay between the two catalytic processes that results in the observed catalytic efficiency.<sup>20,21</sup> That is, the proton transfer enhances the electrophilicity of the anomeric carbon enough to render the nucleophilic attack viable. *Vice versa*, the accumulating negative charge on the leaving exocyclic oxygen renders proton transfer from a weak acid favorable, as is confirmed computationally.<sup>12,13</sup>

At the core of both the pH-dependent activity and catalytic efficiency of Bcx lies the ability of Glu78 and Glu172 to stabilize positive charge in the oxocarbenium-like transition states. The  $pK_a$  values of these residues largely determine these experimental characteristics.<sup>11</sup> It would therefore be extremely useful to be able to tune their  $pK_a$  values independently. Unfortunately the repertoire of 20 common proteinogenic amino acids does not enable this through simple mutagenesis, though it has allowed probing of charge placement.<sup>21</sup> Unnatural amino acids provide a promising alternative, particularly 4-fluoro and 4,4-difluoro glutamic acid (Glu<sub>F</sub> and Glu<sub>FF</sub> respectively), since fluorine is the most electronegative element, yet small enough to minimize steric burden within the active site.<sup>22</sup> By analogy to fluoro- and difluoroacetic acid, 4-fluoro substituents in glutamic acid are expected to lower the  $pK_a$  value of the sidechain carboxylic acid groups by roughly 2 and 3 units, respectively.

The specific introduction of Glu<sub>F</sub> and Glu<sub>FF</sub> into the active site of Bcx is by no means trivial. Whereas fluorinated aromatic amino acids can be introduced via hijacking of amber codons,<sup>23,24</sup> it has thus far not proven possible to develop a tRNA/amino acyl synthetase pair that can distinguish between glutamic acid and its 4-fluorinated derivatives (P. Schultz, Pers. Comm.). We have found that the natural translation apparatus of *E. coli* incorporates Glu<sub>F</sub> and Glu<sub>FF</sub> at a significant level in place of Glu (unpublished results). Although wild type Bcx contains only two Glu residues, this approach would still preclude individual modification of the catalytic nucleophile or general acid/base residue. We therefore chose a semi-synthetic route to access Glu<sub>F</sub> and Glu<sub>FF</sub> ‘mutants’ at the position of the catalytic nucleophile of Bcx. This route involved introduction of the unnatural amino acid into a short synthetic peptide, followed by native chemical ligation with a bacterially expressed counterpart to form a full-length functional enzyme containing the desired modification.<sup>25–27</sup>

While synthetic routes for both 4-fluoroglutamic acid<sup>28–30</sup> and 4,4-difluoroglutamic acid<sup>31–33</sup> have been established, to the best of our knowledge there is no report of the site-selective incorporation of these unnatural amino acids into a peptide or an active enzyme. In this manuscript we describe the methodology we developed to synthesize these molecules, as well as the kinetic characterization of resultant Bcx constructs carrying 4-fluoro- and 4,4-difluoroglutamic acids as their catalytic nucleophile. These studies revealed substantial effects of the modifications upon the pH-dependent activity of Bcx and upon stabilization of the oxocarbenium ion-like transition states.

## Experimental Section

## Results and Discussion

Circular permutant cpP75 allows semisynthesis of Glu78 variants.

Development of a strategy to introduce fluoroglutamic acids into position 78 of Bcx via native chemical ligation of a synthetic peptide and a recombinant truncated protein required several limitations to be taken into account. Firstly, the synthetic peptide needs to be < 15 residues. Even though longer peptides are often accessible via solid phase peptide synthesis, the very hydrophobic nature of the residues flanking Glu78 and their inclination to form insoluble aggregates limits the size that can be reasonably assembled. Indeed, these properties severely hampered the synthesis, purification and characterization of the peptides in this study. Consequently, the site of modification needs to be close to one terminus of the final protein. Fortunately, Bcx is very tolerant towards circular permutation, and a number of active "circular permutants" (cp) have been characterized.<sup>34</sup> The newly generated termini of those circular permutants primarily lie in the loops between the  $\beta$ -strands of the  $\beta$ -jellyroll fold of Bcx.

The second limitation arises from a fundamental requirement of native chemical ligation: The N-terminal component needs to enter the ligation as a C-terminal thioester. Despite tremendous effort on our part, it did not prove possible to generate a thioester derivative of any truncated, recombinantly expressed Bcx fragment since such species cannot adopt a native fold and are highly insoluble in aqueous solution. This ruled out conventional approaches using intein systems.<sup>35</sup> Various chemical approaches to the generation of C-terminal thioesters or hydrazides<sup>36,37</sup> failed also since the long reaction times (> 24 h), elevated temperatures or low pH conditions caused Bcx to either aggregate or hydrolyze.

Consequently, the synthetic peptide needed to be the N-terminal partner in the native chemical ligation reaction and the counterpart expressed protein fragment needed to have an N-terminal cysteine that ends up proximal to the site of modification, Glu78, in the final reconstructed circular permutant (Fig. 1; wt numbering is used throughout for consistency). We generated several circular permutants with their N-termini in the loop near Glu78 and identified cpP75 (i.e., the new N-terminus is Pro75 and the new C-terminus is Ser74, with Ala1-Trp185 linked via a diglycine) as the most promising candidate (data not shown). A suitable ligation site compatible with the size of the synthetic peptide was then required. Fortunately, Bcx has no cysteines, and thus the simplest approach was to mutate a solvent-exposed threonine or serine. We chose Thr87 over Ser84, since the former is preceded by a Gly (facilitating fast ligation), whereas the latter is preceded by Asp, which renders thioesterification and ligation of the peptide impossible.<sup>38</sup>

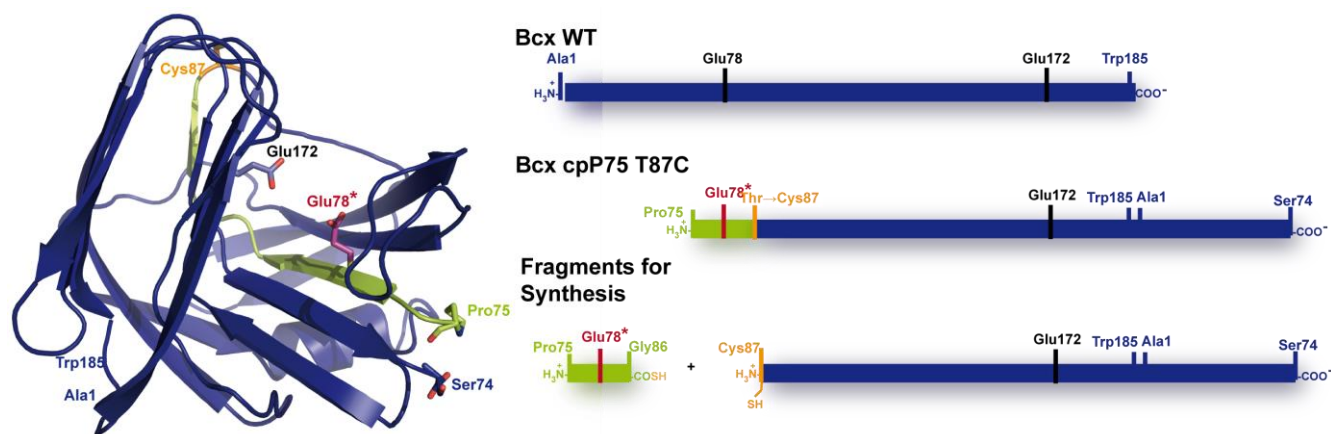


Figure 1: Schematic representations (left, 3D model based on PDB entry 3LB9; right, sequence) of the Bcx construct designed to incorporate an unnatural amino acid at the position of the catalytic nucleophile. The circular permutant Bcx cpP75 T87C (Bcx<sup>cp</sup>, cartoon) is formed by ligation of a 12-mer synthetic peptide (green) containing Glu<sub>FF</sub> or Glu<sub>FF</sub> (Glu78\*, magenta) with a suitably truncated recombinant protein (blue) carrying an N-terminal cysteine. Ligation site (Cys87, orange), N- and C-termini and catalytic residues are represented by stick models.

We recombinantly expressed the resultant control enzyme Bcx cpP75 T87C (henceforth abbreviated as Bcx<sup>cp</sup>). Compared to Bcx<sup>wt</sup>, this protein was produced in *E. coli* at lower, albeit acceptable, expression yields and exhibited reduced thermal stability and catalytic efficiency ( $k_{cat}/K_M = 33\%$  of Bcx<sup>wt</sup>, Table 1). Otherwise the variant behaved like the wild type enzyme in terms of long-term stability and substrate specificity. These findings are in line with those on the previously characterized circular permutants.<sup>34</sup> We therefore set out to semi-synthesize this enzyme by ligating the peptide hydrazide P<sub>75</sub>LIEYYVDSWG<sub>86</sub>-N<sub>2</sub>H<sub>3</sub> with the recombinant fragment Bcx cpP75 T87C  $\Delta$ 75–86 (henceforth Bcx<sup>cp</sup>  $\Delta$ 75–86).

Successful expression of the recombinant fragment Bcx<sup>cp</sup>  $\Delta$ 75–86 in *E. coli* required iterative optimization of the first ten codons by silent mutations (Supporting Information), This presumably prevented the 5'-end of the mRNA derived from the wt sequence from forming stable secondary structures that impeded initiation of the translation process. The expression product was exclusively found in the insoluble fraction of the cell lysate, as expected given that the truncated polypeptide is unable to adopt its native fold. The insolubility of the product unfortunately prohibited its purification. Even though the truncation fragment could be solubilized in strong denaturants such as 6 M guanidinium chloride or 8 M urea at concentrations up to 10 mg/mL, prolonged (> 24 h) handling in solution, mechanical stress, or changes in ionic strength or pH resulted in its aggregation to form a transparent gel. We therefore decided to work with the crude protein (~75% pure judged by SDS PAGE) contained in inclusion bodies that had been thoroughly washed to

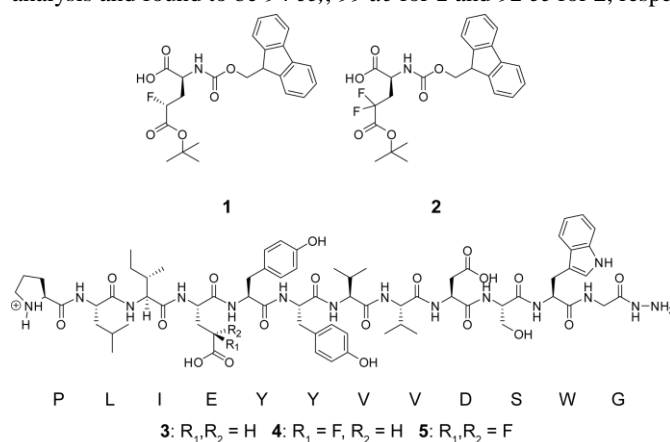
remove cell debris. To characterize the resulting sample, we performed a digestion with Lys-C. Subsequent MALDI TOF analysis of the digested product exclusively showed the expected mass of the N-terminal peptide C<sub>75</sub>YRPTGTYK among possible N-terminal peptides. This indicated that the majority of the expression product contained the desired unmodified N-terminal cysteine residue.

We synthesized the synthetic peptide hydrazide **3** (Scheme 2), which can be converted into an active thioester *in situ*, by using standard Fmoc strategy and a hydrazinyl carboxylate-modified 4-hydroxybenzyl (PHB) resin.<sup>39</sup> The peptide hydrazide was converted into a transient mercaptophenyl acetic acid (MPAA) thioester by oxidation and subsequent addition to a solution containing MPAA as a thiol catalyst in 6 M guanidinium chloride buffer. Even though the ligation with Bcx<sup>cp</sup> Δ75–86 was rapid, conversion halted after 1–2 hours reaction time at ~50% of the protein precursor in all our experiments, judged by comparing the intensity of the bands on the gel. Possibly the N-terminus is blocked in a significant portion of the polypeptides, either by chemical modification or aggregation. Since separation of unfolded product and the remaining precursor is impractical, we directly subjected the reaction mixture to refolding.<sup>40</sup> Our reasoning was that only the ligation product would be able to fold correctly and remain in solution, whereas any nonreactive protein aggregates would precipitate and can be removed by centrifugation. After desalting and concentration of the refolded product, cation-exchange chromatography yielded 300 μg of pure, soluble active enzyme. This was an 11% yield relative to the protein fragment used. As expected, the semi-synthetic Bcx<sup>cp</sup> exhibited the same characteristics and catalytic properties as its recombinant counterpart (data not shown). Having established the applicability of our semi-synthetic approach, we moved on to introduce the fluoroglutamic acids at position 78.

### Synthesis of optically pure fluoroglutamic acid building blocks.

The optimized large-scale synthesis of orthogonally protected, optically pure *N*-Cbz-δOtBu-L-4,4-difluoroglutamic acid from chlorodifluoroacetic acid published by Miller *et al.*<sup>33</sup> proved straightforward in our hands, with an overall yield of 11%. Exchange of the amine protection group (Cbz) for Fmoc to produce building block **2** was accomplished using standard protocols (Supporting Information).

Unprotected 4-fluoroglutamic acid is commercially available as a mixture of all four stereoisomers from Synthequest Labs (Fig. S-1), and thus we used this as a precursor for building block **1**. The orthogonal protection and kinetic resolution of this mix presented two possible complications that were not an issue for **2**: the additional stereocenter and the chemoselective protection of the side-chain carboxylate, which was not expected to be as well discriminated from the α-carboxy group in **1**. However, to our surprise, the methodology of orthogonal protection developed by Miller *et al.* for the 4,4-difluoro derivative was applicable to the 4-fluoroglutamic acid with only minor modifications (Supporting Information). Furthermore, during kinetic resolution, the *B. subtilis* protease employed to selectively hydrolyze the α-methyl ester of the L-isomers in the mixture was also found to prefer the *L-erythro* over the *L-threo* isomer (Fig. S-3). This allowed isolation of the optically pure Cbz-protected precursor, which was reprotected with Fmoc to yield **1**. The integrity of the L-configuration in **1** and **2** was confirmed by modification with Marfey's Reagent and subsequent HPLC analysis and found to be 94 *ee.*, 99 *de* for **1** and 92 *ee* for **2**, respectively.



**Scheme 2: Fluoroglutamic acid building blocks and synthetic peptides prepared for assembly of the modified enzymes. Optically pure and orthogonally protected *threo*-L-4-fluoroglutamic acid (**1**) and L-4,4-difluoroglutamic acid (**2**) were introduced into the 12-mer peptide hydrazides (**4,5**) by Fmoc-based solid phase peptide synthesis.**

### Synthesis and characterization of fluoroglutamic acid-containing peptides.

Successful solid phase peptide synthesis of the fluoroglutamic acid-containing peptide hydrazides **4** and **5** required modifications to the standard procedure used to obtain **3**. Of the two building blocks, only **1** tolerated the standard coupling and Fmoc deprotection conditions without notable side reactions. In contrast, the 4,4-difluoro glutamic acid building block **2** exhibited a number of fatal side reactions, most notably fast formation of a pyroglutamate during deprotection with piperidine, DBU and similar reagents that are commonly used for Fmoc deprotection (Supporting Scheme S-2). Efficient elongation of 4,4-difluoroglutamic acid could only be achieved by use of the milder base piperazine, supplemented with 0.1 M HOBt as acidic modifier, and keeping deprotection times under 5 min with immediate coupling of the subsequent residue. This protocol yielded peptide **5** of a satisfactory purity (Supporting

1 Fig. S-5). However, it should be noted that we found it impossible to introduce **2** into a peptide bearing a Gly residue next to Glu<sub>FF</sub>  
2 (as is the case with the sequence around the Bcx general acid/base catalyst, Glu172). In this case glutarimide formation during solid  
3 phase peptide synthesis diminished the yield. Even when glutarimide formation was prevented by tedious introduction of dimethox-  
4 ybenzyl (Dmb) backbone protection of the Gly amide, the peptide cleaved at various backbone amides around Glu<sub>FF</sub> during depro-  
5 tection in TFA solution (Supporting Fig. S-9). With the bulky, hydrophobic residues flanking Glu78 however, no such side reactions  
6 were observed for peptide **5**.

7 Modifications to our method were also needed to generate the C-terminal hydrazide. We had found that 2-3 rounds of coupling  
8 with 5 eq. Fmoc amino acid per residue were necessary to obtain **3** in satisfactory purity, probably due to the noted hydrophobicity  
9 of the sequence. However, such large excesses would have been too wasteful given our limited supply of building blocks **1** and **2**.  
10 Consequently we moved to the use of a TentaGel resin with low (0.2 mmol/g) substitution to facilitate synthesis. Unexpectedly, the  
11 well-established hydrazinyl-carboxylate-PHB linker used to generate a C-terminal hydrazide<sup>39</sup> proved to be unstable on this resin,  
12 resulting in very low yields and a large share of carboxy-terminated product. We therefore resorted to a protocol recently described  
13 by Bello *et al.*<sup>41</sup> in which a classic carboxyl-linked peptide is assembled on a TentaGel PHB resin. The protected, resin-linked peptide  
14 is then treated with hydrazine solution, resulting in selective cleavage of the linking ester to form a C-terminal hydrazide. In our  
15 hands, treatment with anhydrous hydrazine in THF resulted in a cleavage yield of > 80%. Fortunately, when treatment times were  
16 kept short (< 12 h) and fresh anhydrous reagent was used, no hydrazinolysis of the highly electrophilic sidechain ester of 4,4-glutamic  
17 acid was observed. Peptide hydrazides **4** and **5** were purified by reversed-phase HPLC and their identities confirmed by MALDI TOF  
18 MS and homonuclear NOESY and TOCSY <sup>1</sup>H-NMR spectroscopy.

#### 19 Semisynthesis of Bcx *cp*P75 Glu<sub>F</sub>78 and Glu<sub>FF</sub>78.

20 We subjected peptide hydrazides **4** and **5** to native chemical ligation with Bcx<sup>*cp*</sup> Δ75–86 in the same fashion as with peptide **3**. The  
21 two peptides could only be dissolved up to 0.5 mM in the 6 M guanidinium chloride buffer at pH 3.5 required to convert the hydrazide  
22 to a thioester. The ligation nonetheless proceeded rapidly, terminating in less than one hour (Fig. 2A). However, again for unknown  
23 reasons, only ~ 30% of the precursor protein was consumed as judged by SDS PAGE, even though the peptide was provided in 20-  
24 fold excess over the protein fragment. The reaction solution was subjected to refolding after 6 h and the folded enzymes were isolated  
25 and purified as described previously.<sup>40</sup> Following this protocol, 50 μg of each purified enzyme was obtained per synthesis. The  
26 identities of Bcx<sup>*cp*</sup> Glu<sub>F</sub>78 and Bcx<sup>*cp*</sup> Glu<sub>FF</sub>78 were confirmed by high resolution ESI MS of the intact proteins (Figure 2B and C) and  
27 activity confirmed by measurement using the substrate 2,5-dinitrophenyl β-xylobioside.  
28  
29  
30  
31  
32  
33  
34  
35  
36  
37  
38  
39  
40  
41  
42  
43  
44  
45  
46  
47  
48  
49  
50  
51  
52  
53  
54  
55  
56  
57  
58  
59  
60

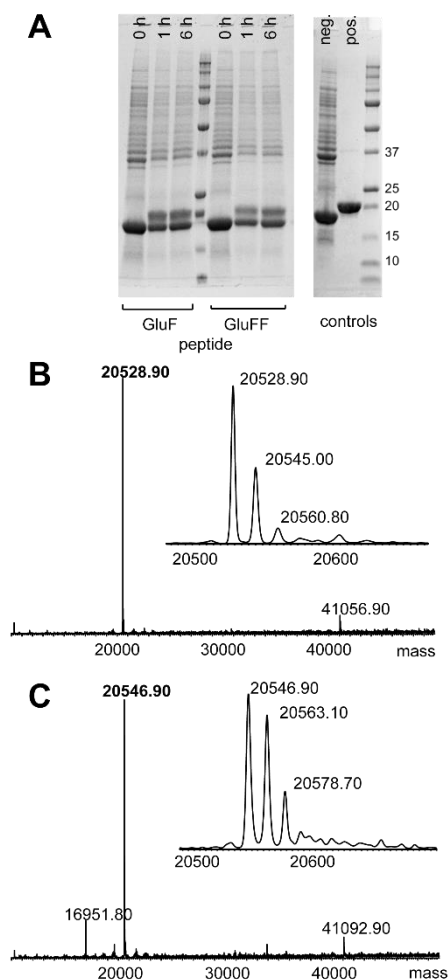


Figure 2: Protein semisynthesis and characterization of Bcx cpP75 Glu<sub>F</sub>78 T87C and Bcx cpP75 Glu<sub>FF</sub>78 T87C. (A) Progress of the native chemical ligation monitored by SDS PAGE. Intact protein ESI MS spectra of the refolded and purified products carrying (B) Glu<sub>F</sub>78 (calc. 20,529, found 20,529) and (C) Glu<sub>FF</sub>78 (calc. 20,547, found 20,547). Additional signals in the expanded insets are attributed to methionine oxidation.

Bcx cpP75 Glu<sub>F</sub>78 and Bcx cpP75Glu<sub>FF</sub>78 show a shift in pH-dependent activities.

The first step in the kinetic characterization of these novel forms of the enzyme was to determine the impact of the substitution of Glu78 by Glu<sub>F</sub> and Glu<sub>FF</sub> on pH-dependent activity. Since the modifications lower the pK<sub>a</sub> values of the fluorinated carboxylic acid they therefore should reduce the share of protonated species at a given pH value, potentially changing the bell-shaped pH vs. activity profile. To explore this the pH profiles (Figure 3) were derived by measuring the second order rate constants ( $k_{cat}/K_M$ ) for hydrolysis of the fluorogenic substrate 6-chloro-4-methylumbelliferyl  $\beta$ -xylobioside (CIMU-X<sub>2</sub>) at 13 pH values. In control experiments, we confirmed that all three enzymes were stable over the assay time used at each pH value (data not shown). As expected, the pH profile of Bcx<sup>cp</sup> carrying Glu as nucleophilic residue was essentially identical to that of Bcx<sup>wt</sup>, with a maximum at pH 6, a pK<sub>a</sub> value of 4.7 attributed to the nucleophile (left hand inflection point of Figure 3A) and a pK<sub>a</sub> value of 7.1 attributed to the acid/base (Glu172). In comparison, the pH profiles of Glu<sub>F</sub>78 (Figure 3B) and Glu<sub>FF</sub>78 (Figure 3C) exhibited strong shifts in maxima and both inflection points towards more acidic pH values, with the difluoro variant undergoing slightly greater perturbations. At least for the nucleophile, this is expected and consistent with the relative sidechain pK<sub>a</sub> values of free Glu, Glu<sub>F</sub> and Glu<sub>FF</sub>. However, it is quite possible that some other ionization equilibria within the proteins at these relatively acidic conditions resulted in the observed pH-profile changes.

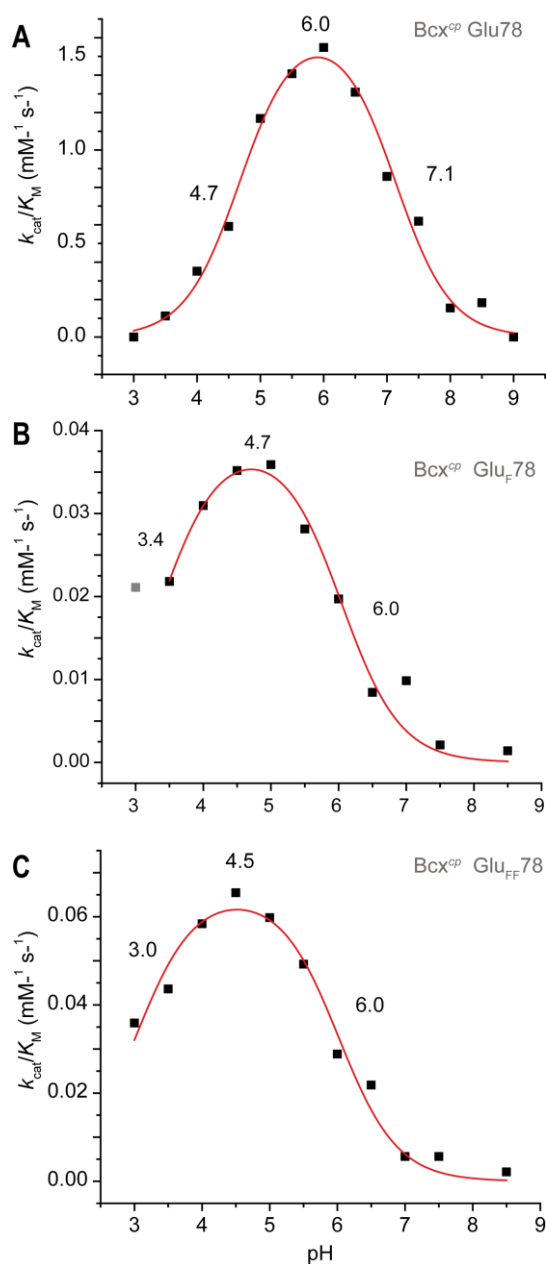


Figure 3: pH-activity profiles for hydrolysis of CIMU-X<sub>2</sub> by Bcx<sup>cp</sup> in its unmodified (Glu78, **A**) and modified forms (Glu<sub>F</sub>78, **B** and Glu<sub>FF</sub>78, **C**). Inflection points and maxima resulting from fitting a double-ionization model to the profiles (red) are indicated at the respective positions.

Interestingly, the pK<sub>a</sub> value attributed to the unmodified acid/base residue Glu172 (right hand inflection points in Figure 3) also shifted to more acidic values in the fluorinated enzymes. This was not expected. However, as seen in previous measurements of active site residue pK<sub>a</sub> values in Bcx, the ionizations are closely coupled.<sup>11</sup> Consequently modification of the acidity of Glu78 is certain to alter the interactions between these residues, and thus the pK<sub>a</sub> value of Glu172, either electrostatically or through subtle conformational perturbations of a tightly linked network of active site residues. For example, the ablation of the charge on Glu78 by mutation to Gln reduces the pK<sub>a</sub> of Glu172 by 2.5 units.<sup>11</sup> Thus a drop of approximately one unit in response to a reduction in partial negative charge on Glu78 upon fluorination is perhaps quite reasonable.

Introduction of Glu<sub>F</sub> and Glu<sub>FF</sub> at position 78 does not alter the rate-determining step.

The overall catalytic efficiencies ( $k_{cat}/K_M$ ) of the fluorinated enzymes are ~25-40 times lower than that of their unfluorinated counterpart at their respective pH maxima. This raises the question of which step is now rate-limiting in the two cases. As noted earlier, for the wild type enzyme, the glycosylation step is rate-limiting in  $k_{cat}$  for aryl glycoside substrates.<sup>42</sup> Further, it is generally expected that glycosylation is rate-limiting in  $k_{cat}/K_M$  for most retaining glycosidases, including Bcx since this represents the first irreversible step.<sup>21</sup> In theory, one might expect that the glycosylation step should remain rate-limiting after lowering the pK<sub>a</sub> value of Glu78 by

fluorination, since this reduces nucleophilicity. By the same token, the deglycosylation step should be accelerated since the fluoroglutamic acid will be a better leaving group than the natural residue.

To test whether this general trend is indeed followed, we studied a reaction in which the two steps are clearly separated. This reaction involved the formation and then the hydrolysis of the 2-fluoroxyllobiosyl-enzyme using the covalent probe 2,4-dinitrophenyl 2-deoxy 2-fluoro- $\beta$ -xylobioside (2,4DNP-2FX<sub>2</sub>). In this probe the electron-withdrawing fluorine at the 2-position of the proximal xylose destabilizes both oxocarbenium-ion-like transition states, slowing both steps. However, the excellent leaving group DNP ensures that the glycosylation step is fast enough for the intermediate to accumulate in Bcx<sup>wt</sup>.<sup>15</sup> If our prediction is correct, inactivation kinetics should be markedly slowed in the Glu<sub>F</sub>78 and, even more so, the Glu<sub>FF</sub>78 variants, while turnover of the covalent intermediate (reactivation) should be faster.

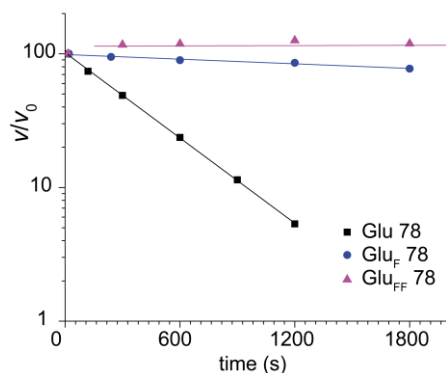


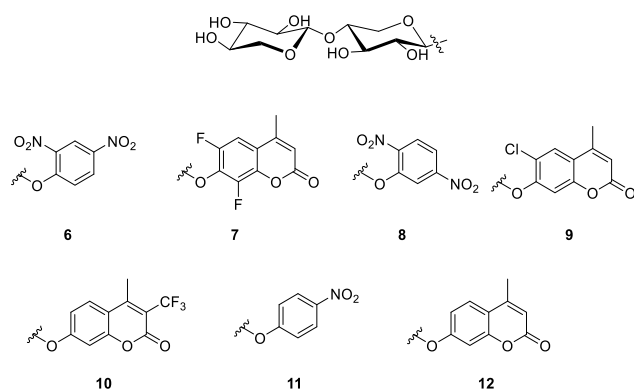
Figure 4: Inactivation of the control enzyme (Bcx<sup>cp</sup> with Glu78) and the two modified enzymes by 5 mM 2,4DNP-2FX<sub>2</sub>.

As shown in Figure 4, inactivation was indeed 20 times slower for the monofluoro glutamic acid variant with Glu<sub>F</sub>78 than for the Glu78 Bcx<sup>cp</sup>. No reaction was seen over 30 minutes with the Glu<sub>FF</sub>78 enzyme. The 20-fold drop in inactivation rate constant is consistent with the ~40-fold lower  $k_{\text{cat}}/K_M$  value for CIMU-X<sub>2</sub> hydrolysis by the Glu<sub>F</sub>78 variant versus the Glu variant (Fig. 3) and confirms a slower glycosylation step.

Reactivation of Bcx<sup>wt</sup> (the deglycosylation step) occurs with a rate constant of  $k_{\text{react}} = 0.0021 \text{ min}^{-1}$ , corresponding to a half-life for the 2-fluoroxyllobiosyl enzyme of  $t_{1/2} = 330 \text{ min}$ .<sup>15</sup> We therefore attempted to measure the rate of reactivation for the Glu<sub>F</sub>78 enzyme, which could be partially inactivated. We first incubated it with a high inactivator concentration (5 mM) for a prolonged time (6 h), and then removed the free inactivator from the enzyme by rapid filtration on a spin filter (MWCO 10,000) at low temperature (4 °C). However, by the time this had been completed, the enzyme had regained activity. Although this precluded the opportunity to measure reactivation kinetics, this observation demonstrates that the half-life for reactivation was considerably less than the 330 min. measured for Bcx<sup>wt</sup>. These studies therefore confirmed predictions concerning the effects of fluorination on the rates of the individual steps. This set the stage for further kinetic studies to probe the structure of the glycosylation transition state.

Lowering the  $pK_a$  value of Glu78 breaks the concerted nature of catalysis in the glycosylation step.

To probe the effects of nucleophile fluorination on the structure of the glycosylation transition state we measured kinetic parameters for hydrolysis of a set of aryl xylobioside substrates with aglycones of differing leaving group ability. This allowed us to vary both the “pull” of the leaving group and the “push” of the nucleophile, and to do so at a pH that is optimal for each enzyme form. We carried out these studies using the seven  $\beta$ -1,4-linked xylobioside substrates shown in Scheme 3, for which the conjugate acids of the aglycones cover a  $pK_a$  range of 4.2 to 7.8 (Table 1). Since the  $pK_a$  values of the acid/base catalyst Glu172 lie between 6 and 7 in our enzyme variants (Figure 3) we used four substrates (6-9) that hydrolyze without general acid catalysis (because the leaving group  $pK_a$  is lower than that of the general acid). In contrast, three substrates (10-12) potentially require general acid assistance.



**Scheme 3:** The aryl xylobioside substrates used in kinetic characterization of Bcx constructs modified at position 78 by fluoroglutamic acid derivatives.

**Table 1:** Measured kinetic constants for Bcx constructs carrying either Glu, Glu<sub>F</sub> or Glu<sub>FF</sub> at position 78. Assays were conducted at 30 °C and at pH 6.0 (Bcx<sup>cp</sup> Glu78), 5.0 (Bcx<sup>cp</sup> Glu<sub>F</sub>78) and 4.5 (Bcx<sup>cp</sup> Glu<sub>FF</sub>78). Standard deviation of the last significant digit is given in brackets. \*Some substrates exhibit  $K_M$  values far above their solubility limit, and therefore individual, isolated kinetic constants could not be determined (n.d.). However, second-order rate constants could be obtained at  $[S] \sim 0.1K_M$ .

Substrate Aglycone $pK_a$	Position 78	$K_M$ (mM)	$k_{cat}$ (s <sup>-1</sup> )	$k_{cat}/K_M$ (mM <sup>-1</sup> s <sup>-1</sup> )
<b>6</b> (2,4-DNP) 4.2	Glu	1.0(0)	14(0)	13.9(5)
	Glu <sub>F</sub>	2.2(3)	1.2(1)	0.52(7)
	Glu <sub>FF</sub>	1.5(1)	1.8(1)	1.2(1)
<b>7</b> (F <sub>2</sub> -MU) 4.7	Glu	21(2)	n.d.	2.9*
	Glu <sub>F</sub>	>20	n.d.	2.2*
	Glu <sub>FF</sub>	>20	n.d.	2.2*
<b>8</b> (2,5-DNP) 5.2	Glu	0.85(9)	7.7(5)	9.0(15)
	Glu <sub>F</sub>	0.9(2)	0.19(1)	0.22(6)
	Glu <sub>FF</sub>	1.1(2)	0.20(1)	0.18(3)
<b>9</b> (Cl-MU) 6.0	Glu	1.7(3)	9.8(7)	5.8(9)
	Glu <sub>F</sub>	1.4(3)	0.11(1)	0.08(1)
	Glu <sub>FF</sub>	0.83(6)	0.060(1)	0.072(5)
<b>10</b> (CF <sub>3</sub> -MU) 7.0	Glu	1.3(2)	0.55(4)	0.42(7)
	Glu <sub>F</sub>	3.1(2)	0.30(1)	0.097(7)
	Glu <sub>FF</sub>	3.5(2)	0.30(1)	0.086(5)
<b>11</b> (pNP) 7.2	Glu	9.6 (85)	n.d.	2.2*
	Glu <sub>F</sub>	>20	n.d.	0.17*
	Glu <sub>FF</sub>	>20	n.d.	0.063*
<b>12</b> (MU) 7.8	Glu	11(2)	2.5(3)	0.090*
	Glu <sub>F</sub>	9.2(16)	0.55(7)	0.068*
	Glu <sub>FF</sub>	27(6)	1.2(3)	0.052*

The steady state kinetic data shown in Table 1 revealed that, for each individual substrate, similar  $K_M$  values were measured for all three Bcx<sup>cp</sup> forms. Thus, the introduced fluorine modifications of Glu78 did not interfere significantly with substrate binding. The same is not true when comparing the  $K_M$  values for each individual enzyme with the seven substrates. Rather, these values fell into two regimes, with the majority around ~2 mM, while the  $K_M$  values of **7**, **11** and **12** were >10 mM. This suggested that the aglycone

structure affected the binding behavior significantly. As a consequence, Brønsted plots of  $\log k_{\text{cat}}$  or  $\log k_{\text{cat}}/K_{\text{M}}$  versus aglycone  $\text{p}K_{\text{a}}$ , while showing correlations (Figure 6A), have considerable scatter that limited their utility or at least masked clear interpretation (Supporting Fig. S-10). Similar scatter was also seen in the previous such study on  $\text{BcX}^{\text{wt}}$ .<sup>14</sup>

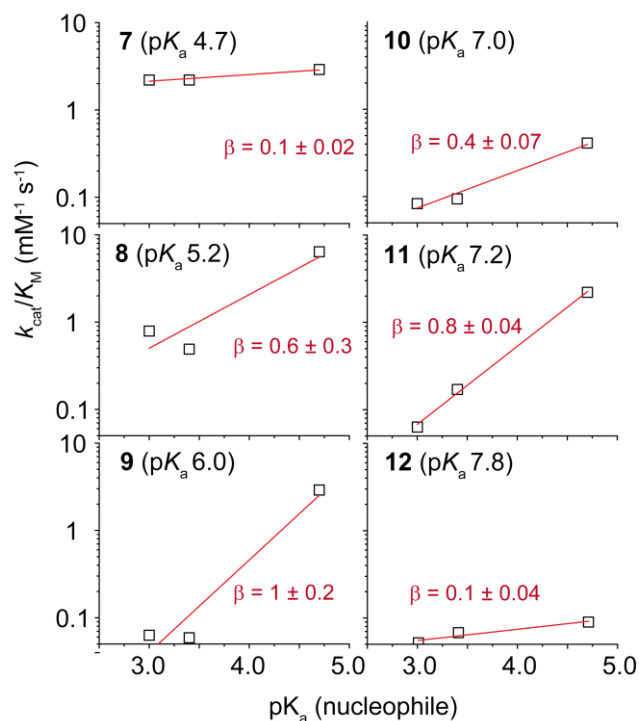


Figure 5: Selected Brønsted plots illustrating varying sensitivity to the nucleophile  $\text{p}K_{\text{a}}$  value versus the quality of the leaving group (aglycone  $\text{p}K_{\text{a}}$  values in parentheses and fit slopes ( $\beta_{\text{NUC}}$ ) indicated). Left-to-right, the data points in each plot correspond to  $\text{BcX}^{\text{cp}}$  with Glu<sup>FF</sup>, Glu<sup>F</sup> and Glu at position 78.

Alternatively, it is possible to inspect the data from the perspective of changes in the  $\text{p}K_{\text{a}}$  value of the nucleophile at position 78. The sterically minimal changes in nucleophile structure do not seem to affect substrate binding, as indicated by the consistent  $K_{\text{M}}$  values across  $\text{BcX}^{\text{cp}}$  variants processing the same substrate. Assuming that the catalytically optimal structure of the active site is likewise undisturbed, we can compare kinetic parameters across these three enzymes with each substrate individually and sidestep the above issues. Accordingly, we present a set of six 3-point Brønsted plots of  $\log k_{\text{cat}}/K_{\text{M}}$  versus nucleophile  $\text{p}K_{\text{a}}$  value for each substrate (Figure 5). The slopes of these plots ( $\beta_{\text{NUC}}$ ) reflect the sensitivity of the reaction to the nucleophile. This in turn relates to the extent of interaction of the nucleophile with the anomeric center at the transition state of the glycosylation step. Indeed, the plots of the  $\beta_{\text{NUC}}$  values versus substrate leaving group  $\text{p}K_{\text{a}}$  have an interesting biphasic form, peaking around an aglycone  $\text{p}K_{\text{a}}$  of 6 (Fig. 6B). This tells us that for substrates of low or high aglycone  $\text{p}K_{\text{a}}$  values, there is little transition state bond formation between the nucleophile and the sugar anomeric center. In contrast, for substrates with aglycone  $\text{p}K_{\text{a}}$  values around 6, the interaction is substantial.

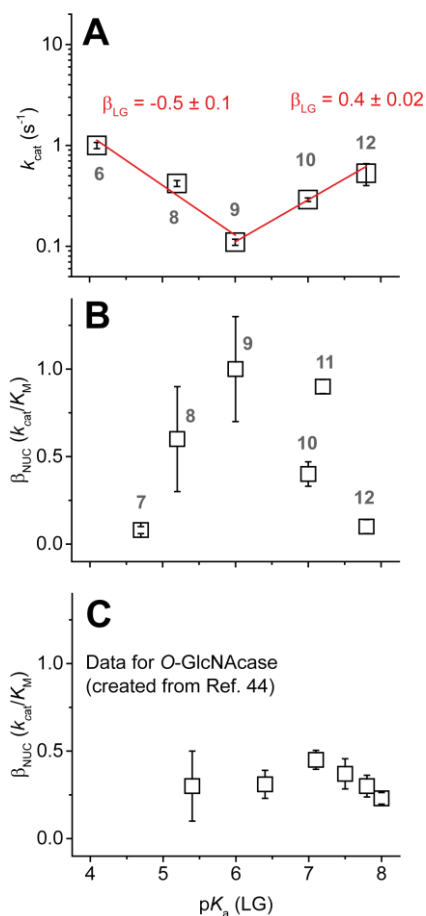


Figure 6: (A) Brønsted plot for Bcx<sup>CP</sup> Glu<sub>F78</sub> reporting a break in  $k_{cat}$  with leaving group (LG) sensitivity  $\beta_{LG}$ . This likely indicates a shift from the single-step mechanism ( $A_N D_N$ ) to a dissociative mechanism  $D_N^{\ddagger} A_N$  (see Fig S-10 for all plots). (B)  $\beta_{NUC}$  values derived from the Fig. 5 plots of  $k_{cat}/K_M$  versus nucleophile  $pK_a$  value for six substrates with differing aglycone  $pK_a$ . (C)  $\beta_{NUC}$  values for the same range of leaving group  $pK_a$  values as reported for human O-GlcNAcase<sup>44</sup>, showing the same trend in decreasing leaving group sensitivity above  $pK_a$  7, where general acid catalysis becomes viable for this enzyme.

Thus substrates, such as **7**, **8** and **9**, that do not require general acid assistance show a progressive need for more nucleophilic push (larger  $\beta_{NUC}$ ) as the aglycone  $pK_a$  increases (poorer leaving group). This observation is in line with a single-step mechanism involving an anionic nucleophile displacing an anionic leaving group ( $A_N D_N$ , Fig. S-11A). Conversely, substrates such as **10** and **12** that require acid catalysis, show decreasing sensitivity towards the nucleophile  $pK_a$  value. Interestingly (although cautiously given the sparse data) this latter phase corresponds to one in which  $k_{cat}$  values for the fluorinated enzymes rise with increasing aglycone  $pK_a$  (Figure 6A and Fig S-10). Such a response implies positive charge accumulation on the glycosidic oxygen at the reaction transition state since relatively electron-donating substituents increase rates. This observation probably reports on almost complete protonation of the glycosidic oxygen at the transition state, with partial fission of the glycosidic bond (Fig. S-11D). In this dissociative mechanism  $D_N^{\ddagger} A_N$ , the nucleophile attacks after the rate-limiting protonation/dissociation, hence the level of concertedness between proton transfer and nucleophilic attack is decreased. Similar behavior was seen in the spontaneous hydrolysis of electron rich aryl glycosides where protonation is facilitated by electron donating substituents on the leaving group.<sup>43</sup>

Thus, it appears that, for our fluorinated enzymes, during enzymatic cleavage of substrates with low aglycone  $pK_a$  values (good leaving groups), the rate-limiting glycosylation reaction occurs without proton donation from the acid/base catalyst and with minimal participation from the enzymatic nucleophile. As the aglycone  $pK_a$  increases towards 6 (thus leaving group ability decreases) nucleophilic participation becomes increasingly important. For substrates with aglycone  $pK_a$  values above 6, acid catalysis can start to contribute to transition state stabilization and consequently protonation of the glycosidic oxygen runs ahead of glycosidic bond cleavage at the transition state. This is reflected in increasing  $k_{cat}$  values with higher aglycone  $pK_a$  values, and indeed this pre-protonation increasingly dominates, with correspondingly decreasing nucleophilic participation (Figure 6A).

Due to the substrate-inherent binding effects that obscure the data (Fig. S-10) these interpretations have to be made with care, even if the observed values of  $\beta_{NUC}$  and  $\beta_{LG}$  are high enough (>0.2) to render any pre-chemical step (like sugar ring distortion) reporting on kinetic constants unlikely. Our findings are also very much in line with a similar study conducted by the Vocadlo group<sup>44</sup>. They demonstrated that the retaining  $\beta$ -N-acetylglucosaminidase OGA acts via a substrate-assisted mechanism in which the neutral carbonyl of the acetamide moiety acts as the nucleophilic catalyst, forming an oxazoline intermediate. In this system the strength of the

nucleophile could be modulated by introduction of fluorines into the amide moiety of the substrate, thereby avoiding laborious modification of the enzyme. The authors observed several regimes in their Brønsted plots. Substrates with good leaving groups (general acid catalysis not required) showed increased sensitivity towards the strength of the nucleophile with decreasing leaving group ability up to the point at which acid catalysis was effective (Figure 6C). Beyond that, in the regime of acid-catalyzed leaving group departure, the same decreasing sensitivity to the strength of the nucleophile with increasing leaving group  $pK_a$  was observed. The authors likewise interpreted this observation as evidence for the formation of a protonated intermediate becoming rate-limiting.

Presumably, the active site of the enzyme has evolved to maximize catalysis of the cleavage of unactivated disaccharide linkages. Accordingly, both acid catalysis and nucleophilic catalysis have been honed to minimize localized charge development. This is achieved by effecting nucleophilic and acid catalysis in a highly concerted fashion, with bond formation from the nucleophile to the anomeric center occurring simultaneously with glycosidic bond cleavage to minimize positive charge development on the sugar ring. Meanwhile proton donation from the acid catalyst occurs with glycosidic bond cleavage to minimize negative charge development on the glycosidic oxygen. By dampening nucleophilic catalysis, we have forced the concerted mechanism to become more asynchronous and dissociative with little nucleophilic participation, thereby exposing these rate dependencies on substrate reactivity.

## Conclusions

In this study we report, for the first time, the site-specific incorporation of fluorinated glutamic acid residues into the active site of an enzyme. Beyond the confirmation of the expected effects on pH-dependent activity, this study has provided unique insights into the fine tuning of nucleophilicity of an anionic nucleophile within an enzyme active site in a sterically and structurally conservative manner. We have shown that the highly concerted nature of the mechanism that has evolved in the wild type enzyme to minimize local charge development on the substrate is achieved by matching the enzymatic nucleophilicity with the acid/base properties of the responsible residue.

## ASSOCIATED CONTENT

**Supporting Information.** Experimental procedures, additional analytical data. This material is available free of charge via the Internet at <http://pubs.acs.org>.

## AUTHOR INFORMATION

### Corresponding Author

\*Stephen G. Withers, Department of Chemistry, University of British Columbia, 2036 Main Mall, Vancouver, B.C., Canada V6T 1Z1; [withers@chem.ubc.ca](mailto:withers@chem.ubc.ca)

## ACKNOWLEDGMENT

We thank Dr. Lars Baumann and Dr. Ian Greig for helpful discussions. We acknowledge financial support from the Natural Sciences and Engineering Research Council of Canada (to L.P.M. and S.G.W.) and a fellowship from the Deutsche Forschungsgemeinschaft (to M.P.K.). Instrument support was provided by the Canada Foundation for Innovation and the British Columbia Knowledge Development Fund.

## ABBREVIATIONS

MPAA, mercapto phenylacetic acid; Bcx, *Bacillus circulans* endo  $\beta$ -1,4-xylanase; *cp*, circular permutant, Bcx<sup>cp</sup>, Bcx *cp*P75 T87C; Bcx<sup>wt</sup>, wild type Bcx; DBU, 1,8-Diazabicyclo(5.4.0)undec-7-ene; Glu<sub>F</sub>, 4-fluoroglutamic acid; Glu<sub>FF</sub>, 4,4-difluoroglutamic acid; MPAA, mercapto phenylacetic acid; TFA, trifluoro acetic acid; CIMU, 6-chloro-4-methylumbelliferyl; DNP-2FX<sub>2</sub>, 2,4-dinitrophenyl 2-deoxy 2-fluoro xylobioside; HOBT, 1-hydroxybenzotriazole; LG, leaving group; NUC, nucleophile, PHB, 4- hydroxybenzyl alcohol; Dmb, dimethoxybenzyl; X<sub>2</sub>,  $\beta$ -xylobioside; DNP, dinitrophenyl; MU, 4-methylumbelliferyl

## REFERENCES

- (1) Wolfenden, R. *Annu. Rev. Biochem.* **2011**, *80*, 645–667.
- (2) Beg, Q.; Kapoor, M.; Mahajan, L.; Hoondal, G. *Appl. Microbiol. Biotechnol.* **2001**, *56*, 326–338.
- (3) Gírio, F. M.; Fonseca, C.; Carvalheiro, F.; Duarte, L. C.; Marques, S.; Bogel-Lukasik, R. *Bioresour. Technol.* **2010**, *101*, 4775–4800.
- (4) Juturu, V.; Wu, J. C. *Biotechnol. Adv.* **2012**, *30*, 1219–1227.
- (5) Sweeney, M. D.; Xu, F. Biomass Converting Enzymes as Industrial Biocatalysts for Fuels and Chemicals: Recent Developments; *Catalysts* **2**, 2012.
- (6) Dumon, C.; Varvak, A.; Wall, M. A.; Flint, J. E.; Lewis, R. J.; Lakey, J. H.; Morland, C.; Luginbühl, P.; Healey, S.; Todaro, T.; DeSantis, G.; Sun, M.; Parra-Gessert, L.; Tan, X.; Weiner, D. P.; Gilbert, H. J. *J. Biol. Chem.* **2008**, *283*, 22557–22564.
- (7) Qian, C.; Liu, N.; Yan, X.; Wang, Q.; Zhou, Z.; Wang, Q. *Enzyme Microb. Technol.* **2015**, *70*, 35–41.
- (8) Koshland, D. E. *Biol. Rev.* **1953**, *28*, 416–436.
- (9) Vocadlo, D. J.; Davies, G. J.; Laine, R.; Withers, S. G. *Nature* **2001**, *412*, 835 EP -.
- (10) Davies, G. J.; Mackenzie, L.; Varrot, A.; Dauter, M.; Brzozowski, A. M.; Schülein, M.; Withers, S. G. *Biochemistry* **1998**, *37*, 11707–11713.

- 1 (11) McIntosh, L. P.; Hand, G.; Johnson, P. E.; Joshi, M. D.; Körner, M.; Plesniak, L. A.; Ziser, L.; Wakarchuk, W. W.; Withers,  
2 S. G. *Biochemistry* **1996**, *35*, 9958–9966.
- 3 (12) Raich, L.; Borodkin, V.; Fang, W.; Castro-López, J.; van Aalten, D. M. F.; Hurtado-Guerrero, R.; Rovira, C. *J. Am. Chem.*  
4 *Soc.* **2016**, *138*, 3325–3332.
- 5 (13) Knott, B. C.; Haddad Momeni, M.; Crowley, M. F.; Mackenzie, L. F.; Götz, A. W.; Sandgren, M.; Withers, S. G.; Ståhlberg,  
6 J.; Beckham, G. T. *J. Am. Chem. Soc.* **2014**, *136*, 321–329.
- 7 (14) Lawson, S. L.; Wakarchuk, W. W.; Withers, S. G. *Biochemistry* **1997**, *36*, 2257–2265.
- 8 (15) Sidhu, G.; Withers, S. G.; Nguyen, N. T.; McIntosh, L. P.; Ziser, L.; Brayer, G. D. *Biochemistry* **1999**, *38*, 5346–5354.
- 9 (16) Whitfield, D. M. *Carbohydr. Res.* **2015**, *403*, 69–89.
- 10 (17) Hartwell, E.; Hodgson, D. R. W.; Kirby, A. J. *J. Am. Chem. Soc.* **2000**, *122*, 9326–9327.
- 11 (18) Kirby, A. J. *Acc. Chem. Res.* **1997**, *30*, 290–296.
- 12 (19) Shan, S.-o.; Herschlag, D. *Proc. Natl. Acad. Sci. U. S. A.* **1996**, *93*, 14474–14479.
- 13 (20) Dean, K. E. S.; Kirby, A. J. *J. Chem. Soc., Perkin Trans. 2* **2002**, 428–432.
- 14 (21) Zechel, D. L.; Withers, S. G. *Curr. Opin. Chem. Biol.* **2001**, *5*, 643–649.
- 15 (22) Berger, A. A.; Völler, J.-S.; Budisa, N.; Koksich, B. *Acc. Chem. Res.* **2017**, *50*, 2093–2103.
- 16 (23) Wang, L.; Brock, A.; Herberich, B.; Schultz, P. G. *Science* **2001**, *292*, 498.
- 17 (24) Wang, L.; Schultz, P. G. *Angew. Chem. Int. Ed.* **2005**, *44*, 34–66.
- 18 (25) Hackeng, T. M.; Griffin, J. H.; Dawson, P. E. *Proc. Natl. Acad. Sci. U. S. A.* **1999**, *96*, 10068–10073.
- 19 (26) Humphrey, J. M.; Chamberlin, A. R. *Chem. Rev.* **1997**, *97*, 2243–2266.
- 20 (27) Muir, T. W. *Annu. Rev. Biochem.* **2003**, *72*, 249–289.
- 21 (28) Kokuryo, Y.; Nakatani, T.; Kobayashi, K.; Tamura, Y.; Kawada, K.; Ohtani, M. *Tetrahedron: Asymmetry* **1996**, *7*, 3545–  
22 3551.
- 23 (29) Konas, D. W.; Coward, J. K. *J. Org. Chem.* **2001**, *66*, 8831–8842.
- 24 (30) Qu, W.; Zha, Z.; Ploessl, K.; Lieberman, B. P.; Zhu, L.; Wise, D. R.; B. Thompson, C.; Kung, H. F. *J. Am. Chem. Soc.* **2011**,  
25 *133*, 1122–1133.
- 26 (31) Ding, Y.; Wang, J.; Abboud, K. A.; Xu, Y.; Dolbier, W. R.; Richards, N. G. J. *J. Org. Chem.* **2001**, *66*, 6381–6388.
- 27 (32) Konas, D. W.; Coward, J. K. *Org. Lett.* **1999**, *1*, 2105–2107.
- 28 (33) Li, Y.; Miller, S. J. *J. Org. Chem.* **2011**, *76*, 9785–9791.
- 29 (34) Reitinger, S.; Yu, Y.; Wicki, J.; Ludwiczek, M.; D'Angelo, I.; Baturin, S.; Okon, M.; Strynadka, N. C. J.; Lutz, S.; Withers,  
30 S. G.; McIntosh, L. P. *Biochemistry* **2010**, *49*, 2464–2474.
- 31 (35) Mootz, H. D. *ChemBioChem* **2009**, *10*, 2579–2589.
- 32 (36) Adams, A. L.; Cowper, B.; Morgan, R. E.; Premdjee, B.; Caddick, S.; Macmillan, D. *Angew. Chem. Int. Ed.* **2013**, *52*, 13062–  
33 13066.
- 34 (37) Kang, J.; Macmillan, D. *Org. Biomol. Chem.* **2010**, *8*, 1993–2002.
- 35 (38) Johnson, E. C. B.; Kent, S. B. H. *J. Am. Chem. Soc.* **2006**, *128*, 6640–6646.
- 36 (39) Fang, G.-M.; Li, Y.-M.; Shen, F.; Huang, Y.-C.; Li, J.-B.; Lin, Y.; Cui, H.-K.; Liu, L. *Angew. Chem.* **2011**, *123*, 7787–7791.
- 37 (40) Kötzler, M. P.; McIntosh, L. P.; Withers, S. G. *Protein Sci.* **2017**, *26*, 1555–1563.
- 38 (41) Bello, C.; Kikul, F.; Becker, C. F. W. *J. Pept. Sci.* **2015**, *21*, 201–207.
- 39 (42) Lawson, S. L.; Wakarchuk, W. W.; Withers, S. G. *Biochemistry* **1996**, *35*, 10110–10118.
- 40 (43) Nath, R. L.; Rydon, H. N. *Biochem. J.* **1954**, *57*, 1.
- 41 (44) Greig, I. R.; Macauley, M. S.; Williams, I. H.; Vocadlo, D. J. *J. Am. Chem. Soc.* **2009**, *131*, 13415–13422.
- 42
- 43
- 44
- 45
- 46
- 47
- 48
- 49
- 50
- 51
- 52
- 53
- 54
- 55
- 56
- 57
- 58
- 59
- 60

1  
2  
3  
4  
5  
6  
7  
8  
9  
10  
11  
12  
13  
14  
15  
16  
17  
18  
19  
20  
21  
22  
23  
24  
25  
26  
27  
28  
29  
30  
31  
32  
33  
34  
35  
36  
37  
38  
39  
40  
41  
42  
43  
44  
45  
46  
47  
48  
49  
50  
51  
52  
53  
54  
55  
56  
57  
58  
59  
60  
**Table of Contents Graphic**